Discussion Paper No. 93

Analysis of Similarity among Surfaces Defined in the Identical Region

Yukio Sadahiro* and Masae Masui**

*Department of Urban Engineering
**Institute of Environmental Studies
University of Tokyo

7-3-1, Hongo, Bunkyo-ku, Tokyo 113-8656, Japan

Phone: +81-3-5841-6273
Fax: +81-3-5841-8521
E-mail: sada@okabe.t.u-tokyo.ac.jp

October 27, 2002

Analysis of Similarity among Surfaces Defined in the Identical Region

Yukio Sadahiro* and Masae Masui**

*Department of Urban Engineering

**Institute of Environmental Studies

University of Tokyo

7-3-1, Hongo, Bunkyo-ku, Tokyo 113-8656, Japan

Phone: +81-3-5841-6273

Fax: +81-3-5841-8521

E-mail: sada@okabe.t.u-tokyo.ac.jp

Analysis of Similarity among Surfaces Defined in the Identical Region

Abstract

This paper develops a method for analyzing the similarity among surfaces defined in the identical region. The method quantitatively evaluates the similarity among surfaces with respect to their spatial configuration, and detects spatial structures shared by the surfaces. The former shows 'to what extent' surfaces are similar, while the latter describes 'how' surfaces are similar. Evaluation of surface similarity is based on mathematical functions that describe the agreement of surfaces at each location and direction. Integrals of the functions with location and direction give quantitative measures of the total similarity among surfaces. The evaluation is followed by the detection of spatial structures shared by the surfaces: α-peak regions, α-pit regions and β-monotonic lines. α-peak and α-pit regions indicate approximate locations where many surfaces have peaks and pits, respectively. β-monotonic lines are line segments on which most surfaces change monotonically in the same direction. These spatial objects reveal the spatial structure shared by surfaces. The method is applied to analysis of the daily market structure of a supermarket in Japan as an empirical study.

The surface is a computational model of scalar field defined in a region. It is used for modeling elevation of the earth's surface (Pike 1988; Hutchinson 1989; Etzelmuller 2000), distribution of geological measures (Isaaks and Srivastava 1989; Cressie 1993; Bailey and Gatrell 1995), population distribution (Bracken 1993; Bracken and Martin 1995), and so forth, in order to perform spatial analysis in GIS environment.

Once a geographical region is given, it often happens that several surfaces are defined in the region. Taking a state of the United States, for instance, we can find spatial datasets representing the distributions of temperature, humidity, and atmospheric pressure, which are typical example of surfaces defined in the identical region. Population distribution also forms a set of surfaces if it is classified by age group. Time-series spatial data, say, daily distribution of nitrogen oxides, can be regarded as surfaces if they are modeled as a set of different layers in GIS.

In analysis of surfaces, we are often interested in the spatial relationship among them. The method of analysis depends on the amount of analysts' knowledge about surfaces. If analysts have little knowledge, they usually perform exploratory spatial analysis to find interesting patterns in the relationship among surfaces. One method is to compare measures or functions that summarize the spatial properties of surfaces such as spatial autocorrelation statistics and geostatistical functions. On the other hand, if analysts have enough knowledge about surfaces, they can perform confirmatory spatial analysis.

Statistical tests are available to confirm their research hypotheses; mathematical models are also useful to understand the relationship among surfaces, such as spatial regression models (Bailey and Gatrell 1995) and bidimensional regression models (Tobler 1994; Nakaya 1997).

In exploratory spatial analysis, analysts often fail to detect spatial patterns in the relationship among surfaces. For instance, if one surface is the mirror image of another surface defined in the same region, they yield the same spatial autocorrelation statistics. Two surfaces different only in location have the same variogram function. It is obviously problematic in exploratory spatial analysis to overlook these kinds of basic differences among surfaces. Though they can easily be detected by visual analysis, it is not realistic to check all the surfaces if there are hundreds or thousands of surfaces.

The main cause of this problem is that analysis is performed in individual surfaces separately (Sadahiro 2001a, 2001b). The spatial information of surfaces is summarized into nonspatial measures or functions before the relationship among surfaces is analyzed; locational information is not explicitly taken into account in analysis of surface relationship. To resolve the problem, this paper proposes a new method for analyzing the relationship among surfaces defined in the identical region. The method focuses on the spatial similarity among surfaces because it is one of the most basic spatial relationships discussed in spatial analysis. The next section describes the background and outline of the

method, which is followed by detailed descriptions in Sections 2 and 3. Section 4 applies the method to analysis of the daily market structure of a supermarket in Japan. Section 5 summarizes conclusions with discussion.

1. BACKGROUND AND OUTLINE OF THE METHOD

Suppose a set of surfaces that represent the population distributions of three age groups in a region, under 20, 20-40, and over 40 (Figure 1). The distributions are globally similar among different age groups. People are clustered in two areas, one in the northwest and the other in the south. Population density smoothly decreases around the peaks of distributions.

Fig. 1. Population distributions of three different age groups in a region.

From a microscopic viewpoint, on the other hand, we find several differences among the surfaces. For instance, the northwest peak is higher than the south peak in groups 1 and 3, while they are almost the same height in group 2. Group 1 people are heavily concentrated in the northwest, while groups 2 and 3 are rather dispersed in this region. Groups 2 and 3 have another peak in the east. Group 3 also has a pit between the peaks in the northwest and south.

Through visual analysis we can easily find similarities and differences among surfaces in this way. This is the first step of exploratory spatial analysis, which is usually followed by more sophisticated spatial analysis including spatial autocorrelation analysis, geostatistical analysis, and spatial modeling.

Visual analysis, however, does not work for a great number of surfaces. It takes considerable time to analyze hundreds of surfaces visually, and it is even practically impossible to detect their similarities and differences. Moreover, since visual analysis is inherently subjective to some extent, it does not provide quantitative measures of similarities and differences among surfaces, which are indispensable for spatial analysis at advanced stages.

Nevertheless, there is no doubt that findings obtained by visual analysis are extremely useful in spatial analysis. Considering this advantage, we develop a new method for analyzing the spatial similarity among surfaces, which is applicable to a great number of surfaces and partly substitutes for the visual analysis mentioned above. The method consists of two steps: evaluation of similarity among surfaces and detection of spatial structures shared by surfaces. Evaluation of surface similarity is based on mathematical functions that represent the agreement of surfaces at each location and direction. This provides us quantitative information about 'to what extent' surfaces are similar, that is, the degree of similarity. The evaluation is followed by the detection of

spatial structures shared by surfaces, which tells us 'how' surfaces are similar. More specifically, the method automatically extracts the global pattern found in visual analysis of Figure 1: similarities in location of peaks and form of their accompanying slopes. These steps are successively explained in the following sections.

2. EVALUATION OF SIMILARITY AMONG SURFACES

Suppose a region S of area A and a set of surfaces represented by scalar functions $F=\{f_1(\mathbf{x}), f_2(\mathbf{x}), ..., f_n(\mathbf{x})\}$. Those surfaces may represent continuous distributions of different types, say, temperature, humidity, and atmospheric pressure, or they may be a set of time-series distributions of the same spatial phenomenon.

To evaluate the similarity among surfaces we use a scalar function called the *slope function* (Sadahiro 2003). The function represents the vertical direction of a surface function at a given location and direction as a binary variable. Let $\mathbf{v}(\theta)$ be the unit vector of angle θ measured counterclockwise from the x-axis ($0 \le \theta < 2\pi$). The gradient of the ith surface function at $\mathbf{x}$ in direction θ is given by the directed differentiation of $f_i(\mathbf{x})$:

$$f_i'(\mathbf{x},\theta) = \nabla f_i(\mathbf{x})\mathbf{v}(\theta). \tag{1}$$

Using $f_i'(\mathbf{x}, \theta)$, we define the slope function of $f_i(\mathbf{x})$:

$$\sigma(\mathbf{x},\theta; f_i) = \begin{cases} 1 & \text{if } f_i'(\mathbf{x},\theta) \ge 0 \\ 0 & \text{otherwise} \end{cases}. \tag{2}$$

The slope function becomes one if the surface ascends at ($\mathbf{x}$, θ); otherwise the

function is zero. Figure 2 shows examples of the slope function in a one-dimensional space.

Fig. 2. Surfaces (upper row) and their slope functions (lower row) in a one-dimensional space. The direction θ is set to the positive direction of the x-axis.

As seen in Figure 2, the slope function is a simplification of surface function. This implies that surfaces of the same slope function are regarded as equivalent. In Figure 2, for instance, Figures 2a and 2b are equivalent with respect to the slope function. Since the slope function emphasizes the spatial aspect of surfaces, it is useful for analyzing their spatial structure. Similar discussion can be found in Okabe (1982).

Using the slope function we evaluate the similarity among surfaces at each location and direction in *S*. A simple method is to consider only two cases: all the surfaces consistently ascend or descend, or some ascend while the others descend. In the former case all the slope functions share the same value, either zero or one; in the latter case some functions are zero while the others are one. Similarity among surfaces is then represented by the *complete agreement function*, a binary function of ($\mathbf{x}$, θ) that indicates whether all the slope functions agree at ($\mathbf{x}$, θ):

$$\eta(\mathbf{x},\theta;F)=\begin{cases}1 & \text{if } \sum_i \sigma(\mathbf{x},\theta;f_i)=0 \text{ or } n\\ 0 & \text{otherwise}\end{cases}. \qquad (3)$$

The complete agreement function is one if and only if all the surfaces share the same slope function value (Figure 3a).

Fig. 3. Agreement functions in a one-dimensional space. (a) Complete agreement function, (b) partial agreement function (μ=0.8), (c) spatially-extended agreement function, (d) generalized agreement function. Small triangles indicate the slope function values.

The definition of complete agreement function, however, is too strict for practical use. The function detects only the complete agreement among surfaces as shown in Figure 3a, which is not so useful in exploratory spatial analysis. To extend the applicability, we relax the evaluation rule in three different ways.

One method is to permit partial agreement among surfaces. This approach is more realistic because it rarely occurs that a great number of surfaces share the same slope function at a given location and direction. We thus consider whether most, not all, of surfaces ascend (descend) at (**x**, θ). This evaluation is mathematically defined by the *partial agreement function*:

$$\eta_P(\mathbf{x},\theta,\mu;F)=\begin{cases}1 & \text{if } \sum_i \sigma(\mathbf{x},\theta;f_i)\le(1-\mu)n \text{ or } \mu n\le\sum_i \sigma(\mathbf{x},\theta;f_i)\\ 0 & \text{otherwise}\end{cases}. \quad (4)$$

The parameter μ is the minimum proportion of surfaces to say that surfaces are similar at

($\mathbf{x}$, θ); the function becomes one if μn out of n surfaces have the same slope function. In Figure 3b, for instance, μ is set to 0.8 so that the partial agreement function becomes one at $\mathbf{x}_2$, though $f_5(\mathbf{x})$ has the different slope function value.

Another extension is to permit locational difference of points that have the same slope function value. Let us recall the surfaces shown in Figure 1. The location of the highest peak is slightly different among the three surfaces, though it is hardly perceptible in the figure. This kind of locational difference is not taken into account in either complete or partial agreement functions. As a result, two congruent surfaces of slight different locations may not be regarded as similar in terms of these functions.

To allow the locational difference, we introduce a locational tolerance r. Let us suppose that $\sigma(\mathbf{x}, \theta; f_j)$, the slope function of $f_i(\mathbf{x})$, is one at ($\mathbf{x}$, θ) while the other slope functions are zero. In this case we search a location within distance r of $\mathbf{x}$ where $\sigma(\mathbf{x}, \theta; f_j)=0$. If we find such a location we consider that all the surfaces are similar at ($\mathbf{x}$, θ). If the slope functions of two surfaces $f_i(\mathbf{x})$ and $f_j(\mathbf{x})$ are one while those of the others are zero, we do the above search for both $f_i(\mathbf{x})$ and $f_j(\mathbf{x})$.

This evaluation is mathematically described as follows. We define a binary function

$$\kappa(\mathbf{x},\theta,r,a; f_i) = \begin{cases} 1 & \text{if } \exists \mathbf{y}, |\mathbf{x}-\mathbf{y}| \le r, \sigma(\mathbf{y},\theta; f_i) = a \\ 0 & \text{otherwise} \end{cases}, \quad (5)$$

where a is a binary variable that takes either one or zero. The binary function $\kappa(\mathbf{x}, \theta, r, a; f_j)$ is one if there is a location within distance r of $\mathbf{x}$ where $\sigma(\mathbf{x}, \theta; f_j)=a$. Using the

function we define the *spatially-extended agreement function*:

$$\eta_s(\mathbf{x},\theta,r;F)=\begin{cases}1 & \text{if } \sum_i \kappa(\mathbf{x},\theta,r,0;f_i)=n \text{ or } \sum_i \kappa(\mathbf{x},\theta,r,1;f_i)=n \\ 0 & \text{otherwise}\end{cases}. \quad (6)$$

The function becomes one, indicating that the surfaces are regarded as similar at (**x**, θ), if all the surfaces share the same slope function value within distance r of **x**.

Let us compare Figures 3a and 3c. In Figure 3a the complete agreement function is zero at $\mathbf{x}_3$, because the slope functions of $f_1(\mathbf{x})$, $f_3(\mathbf{x})$, and $f_5(\mathbf{x})$ are zero while those of $f_2(\mathbf{x})$ and $f_4(\mathbf{x})$ are one. However, if we permit the locational tolerance r as shown in Figure 3c, we can find locations where the slope functions of $f_2(\mathbf{x})$ and $f_4(\mathbf{x})$ are zero. Consequently, the spatially-extended agreement function becomes one at $\mathbf{x}_3$.

Third extension of the complete agreement function is to use a continuous instead of binary function. If $m(>n/2)$ out of n surfaces share the same slope function value at (**x**, θ), it is natural to use m/n as a measure of similarity among the surfaces. This leads to the definition of the *generalized agreement function*:

$$\eta_g(\mathbf{x},\theta;F)=\frac{2}{n}\max\left\{\sum_i \sigma(\mathbf{x},\theta;f_i), n-\sum_i \sigma(\mathbf{x},\theta;f_i)\right\}-1. \quad (7)$$

This function indicates the higher ratio of surfaces of the same slope function value (Figure 3d). If many surfaces either ascend or descend consistently at (**x**, θ), the generalized agreement function shows a large value. The function becomes zero if a half of surfaces ascend and the other half descend. The range of the generalized agreement function is $0\le\eta_g(\mathbf{x}, \theta; F)\le 1$.

The above three extensions can also be combined with each other. For instance, we may further extend the partial agreement function by considering a locational tolerance. Surfaces are regarded as similar if most of them have the same slope function value around a certain location, not necessarily at the same location but in a neighborhood. Both the partial and spatially-extended agreement functions can be defined as continuous functions that represent the higher ratio of surfaces having the same slope function value. These kinds of combinations further extend the means of evaluating surface similarity.

The agreement functions proposed above indicate the spatial variation of the similarity among surfaces. They are in a sense local measures because evaluation is based on the local relationship among surfaces. To evaluate the global similarity, we integrate the agreement functions in *S*, the region in which they are defined. For instance, the *complete* a*greement index* of the surface set *F* is defined by the integral of the complete agreement function $\eta(\mathbf{x}, \theta; F)$ with $\mathbf{x}$ and θ in *S*:

$$a(F) = \frac{1}{2\pi A}\int_{\mathbf{x}\in S}\int_{\theta\in[0,2\pi]} \eta(\mathbf{x},\theta;F)\mathrm{d}\theta\mathrm{d}\mathbf{x}. \qquad (8)$$

The integral is divided by $2\pi A$ to keep the range of the index from zero to one. The complete agreement index, as a result, shows the ratio of the area in *S* where $\eta(\mathbf{x}, \theta; F)=1$. *Partial*, *spatially-extended,* and *generalized* a*greement indices* are also defined similarly. These indices become large if surfaces are similar at a global scale.

3. DETECTION OF SPATIAL STRUCTURES SHARED BY SURFACES

The agreement functions and their integral indices describe 'to what extent' surfaces are similar. They provide us a general view of surface similarity even if a great number of surfaces exist. On the other hand, they do not explicitly show 'how' surfaces are similar. For instance, similarities in location of peaks and form of their accompanying slopes discussed in Figure 1 are not detectable. It is also important in exploratory spatial analysis to find spatial patterns and structures shared by surfaces.

To answer this demand, this section proposes a method for detecting spatial structures shared by surfaces. We discuss two types of spatial objects, both of which characterize the global structure of surfaces: regions in which many surfaces have peaks, and lines on which many surfaces change monotonically in the same direction.

3.1 α-Peak Regions and α-Pit Regions

The *peak region*, a concept proposed in Sadahiro (2003), is a region in which all the surfaces have at least one peak. Sadahiro (2003) uses it to describe the stability of the surface generated by spatial smoothing from a point distribution of uncertain location: each peak region contains at least one peak independently of the location of points.

Though the concept of peak region seems suitable for our objective, its definition is too strict to use in exploratory spatial analysis; it rarely occurs that a great number of

surfaces have peaks in the same small region. Relaxing the definition slightly, we introduce a new concept what we call the *α-peak region.* Unlike the peak region, the α-peak region permits partial inconsistency among surfaces: it contains the peaks of many, not necessarily all, of surfaces. The prefix α is the minimum ratio of surfaces that have peaks in the α-peak region.

There are numerous regions that fit the above definition, some of which are of no use for spatial analysis. In Figure 1, for instance, all the surfaces have peaks in the northwest of the center. We intuitively expect a small α-peak region around there. However, we can also consider larger α-peak regions that contain the peaks of three surfaces. Even the whole region is an α-peak region. Such regions are neither acceptable nor useful in exploratory spatial analysis, because they give little information about the similarity among surfaces, that is, locational similarity of peaks.

To extract only the regions meaningful in spatial analysis, we discuss the desirable properties of α-peak regions. The first property is that the α-peak region is small enough compared with the region in which surfaces are defined. It should be as small as possible to keep its usefulness. To focus only on small regions we determine the maximum size of the α-peak region by the ratio of its area to that of the region in which surfaces are defined. The second property is that the α-peak region has a simple shape. Without this restriction regions of very complicated shapes are permitted (Figure 4), which are also of

no use for spatial analysis. To avoid this we only consider circular α-peak regions.

Fig. 4. A region containing the peaks of seven different surfaces. Though the region is small, its shape is so elongated and complicated that it gives little information about the locational similarity of peaks.

To detect α-peak regions with the properties discussed above, we develop a computational algorithm. Since there are still numerous α-peak regions, the algorithm presents only some important regions to avoid providing excessive and redundant information. The algorithm consists of three steps: detection of peaks in each surface, extraction of α-peak regions, and choice of α-peak regions to be displayed.

Peaks of a surface are detected as follows. We place a square lattice of *m* small cells on the region *S* and choose the cells whose surface value is larger than those of the neighboring cells. Since these cells may contain peaks, we search for a local maximum by a descent method (Fiacco and McCormick 1968; Gill *et al.* 1981) in each cell to specify the exact location of peaks (for details, see Sadahiro, 2002). Though this method does not assure detection of all the peaks of a surface, it fails to detect only small peaks which are not significant in analysis.

The next step is extraction of α-peak regions. We again place a square lattice of *m*'

cells on *S* (Figure 5a). We do not have to use the same lattice as we used in peak detection. At each lattice point we draw a small circle and expand it until it contains the peaks of αn surfaces (Figure 5b). The circles obtained fit the definition of the α-peak region. We then shrink the circles as small as possible, keeping the peaks in their inside (Figure 5c). The shrinkage process is equivalent to the problem of finding the smallest enclosing circles in computational geometry, for which efficient algorithms have been developed (Megiddo, 1983; Preparata and Shamos, 1985; Skyum, 1991). The circles in Figure 5c are considerably smaller than those in Figure 5b, which reflects the first desirable property of the α-peak region discussed earlier. We finally eliminate the circles larger than the maximum size determined in advance.

This method does not assure that no smaller α-peak regions still remain to be extracted. In this sense the α-peak regions extracted by this method are approximate solutions. However, it is not the main objective of exploratory spatial analysis to find 'exact' solutions, which takes a considerable computing time. The above method is practically acceptable with respect to its computational efficiency and expected results as seen in Figure 5.

Fig. 5. Extraction of α-peak regions. (a) Peaks detected in surfaces. The same symbol indicates the peaks of the same surface. Dashed lines indicate the lattice placed for

extraction of α-peak regions. (b) Circles centered at lattice points that contain the peaks of α*n* surfaces (α=1.0). (c) The smallest circles containing the peaks of α*n* surfaces.

As shown in Figure 5c, α-peak regions usually overlap with each other. Regions that share some peaks give us similar information about the location of peaks. To avoid this information redundancy, we finally choose only some important α-peak regions to be displayed. Since smaller regions are more desirable, we arrange α-peak regions by size and extract the smallest region in turn (Figure 6). During the process we eliminate α-peak regions that share some peaks with smaller ones. In Figure 6, from initial sixteen α-peak regions we choose four to be displayed as the output of analysis.

Fig. 6. Choice of α-peak regions to be displayed. (a) Initial α-peak regions. The same symbol indicates the peaks of the same surface. (b) Extraction of α-peak regions in turn. Gray-shaded circles indicate the α-peak regions extracted. The small circle indicated by a dashed line was not extracted because it shares two peaks with the smaller circle on the right. (c) α-peak regions to be displayed.

Computational complexity of the above algorithm is as follows. Detection of peaks in *n* surfaces requires O(*mn*) computing time. Extraction of α-peak regions consists of

two substeps: calculation of circles at lattice points that contain the peaks of α*n* surfaces and shrinkage of the circles as small as possible. Their computing times are of O(*m*'*n* log *n*) and O(*m*'*n*), respectively. Computational complexity of choosing α-peak regions to be displayed is O(*m*' log *m*'). Consequently, in the worst case, the algorithm runs in O(max{*mn*, *m*'*n* log *n*, *m*' log *m*'}) time.

On average, however, the algorithm runs faster. Sorting routines are included in the initial calculation of α-peak regions and the choice of α-peak regions to be displayed. In the above discussion we assume Heapsort or Mergesort algorithm that requires O(*n* log *n*) computing time in the worst case. Quicksort, on the other hand, runs in O(*n*) time on average, while in O(n^2) time in the worst case. Consequently, if we use Quicksort instead of Heapsort or Mergesort, the total computational complexity is O(max{*mn*, *m*'*n*}) on average.

If more than one α-peak region are chosen to be displayed, we determine their ranking by height. Suppose *k* α-peak regions P_1, P_2, ..., P_k in *S*. We first decide the ranking of α-peak regions in individual surfaces by the height of peaks (Figure 7a). If an α-peak region has more than one peak in a surface, the highest peak is considered. Rank is not given to α-peak regions that do not contain any peak. The α-peak region that ranks first in the most surfaces is given the first rank among all the α-peak regions (Figure 7a). Excluding the α-peak region, we again decide the ranking of the remaining *k*-1 α-peak

regions in individual surfaces and choose the α-peak region that ranks first in the most surfaces (Figure 7b). We repeat this process until the ranks of all the α-peak regions are determined (Figure 7c).

Fig. 7. Determination of the ranking of α-peak regions by height. (a) Ranking of α-peak regions $\{P_1, P_2, P_3, P_4\}$ in individual surfaces. The region P_1 is given the first rank because it ranks first in three out of five surfaces. (b) Ranking of the remaining α-peak regions $\{P_2, P_3, P_4\}$. The region P_4 is then given the second rank. (c) The ranking of all the α-peak regions.

As well as the α-peak region, it is often useful to consider the *α-pit region*, a region in which many surfaces have pits. α-pit regions can be easily extracted by turning surfaces upside down and applying the algorithm extracting α-peak regions. Using the α-peak and α-pit regions together, we can describe 'how' surfaces are similar in more detail.

3.2 β-Monotonic Lines

The surfaces shown in Figure 1 have two similarities: the location of peaks and the form of their surrounding slopes. The former is represented as α-peak regions. This

subsection discusses the latter, that is, the similarity in the form of slopes.

The slopes in Figure 1 decrease gradually and monotonically with the distance from peaks. To treat such slopes we introduce another new concept the *β-monotonic line*. The β-monotonic line is a line segment on which many surfaces have the same monotonic trend, either increase or decrease, in the same direction. Similar to the α-peak region, the β-monotonic line permits partial inconsistency among surfaces: if most surfaces decrease monotonically, the others can increase or even fluctuate. β is the minimum ratio of surfaces that share the same trend on the line.

There are numerous line segments that fit the above definition. Recalling Figure 1, we focus on the radial lines extending from the centers of α-peak regions, which represent the slopes accompanied by peaks. We extract radial lines on which many surfaces decrease monotonically with the distance from α-peak regions.

A computational algorithm for detecting β-monotonic lines is as follows. β-monotonic lines are defined for individual α-peak regions separately. Given an α-peak region *P* and a direction φ, we first stand at the intersection of the boundary of *P* and the radial line extending from the center of *P* in direction φ. We move in direction φ while β*n* out of *n* surfaces decrease monotonically on the path. Repeating this process for a set of directions we obtain β-monotonic lines for the α-peak region *P* (Figure 8). Computational complexity of this algorithm is O(*l n* log *n*) in the worst case, where *l* is

the number of directions considered for each α-peak region. On average, however, it runs in O(*ln*) time if we use Quicksort in sorting routines.

Fig. 8. β-monotonic lines in a one-dimensional space. Black and white triangles indicate peaks and pits, respectively. Parameters α and β are both set to 0.8.

Mathematically, extraction of β-monotonic lines can be formalized as an optimization problem by using the slope function. Suppose an α-peak region P and a direction φ measured counterclockwise from the x-axis. Let L be a line segment of direction φ whose one end is on the center of P. We define a binary function $\nu(L; f_i)$ that indicates whether the surface function $f_i(\mathbf{x})$ monotonically decreases on L:

$$\nu(L; f_i) = \begin{cases} 1 & \text{if } \forall \mathbf{x} \in L \setminus P, \sigma(\mathbf{x}, \varphi; f_i) = 0 \\ 0 & \text{otherwise} \end{cases}. \quad (9)$$

Calculation of the β-monotonic line is then formalized as the maximization of the length of L:

$$\max_{\beta n \le \sum_i \nu(L; f_i)} |L \setminus P|. \quad (10)$$

4. EMPIRICAL STUDY

This section empirically analyzes the daily market structure of a supermarket, which is represented as a set of surfaces, in order to test the validity of the method proposed in

the previous sections. The supermarket A, which is a high-class supermarket like Dean & Deluca in the United States, is located in a suburban area of Tokyo, Japan (Figure 9). The supermarket A has a card membership system which offers 5% discount to card holders. The shopping histories of members are stored as a digital dataset with their attributes including name, address, age, and income class.

Fig. 9. Study region.

We borrowed a part of the data from the supermarket company: the daily distribution of cardmembers who shop at the supermarket from May 13 (Mon.) to June 9 (Sun.) in 2002. The data were represented as twenty-eight layers in GIS. To keep the confidentiality of cardmembers, the data were aggregated at *oaza* level, one of the administrative units in Japan.

Figure 10 shows the average number of cardmembers shopping at the supermarket A per day·household. The distribution seems quite natural at a global scale: a unimodal distribution with a monotonic slope. Customers are clustered near the supermarket, and decrease almost monotonically with the distance from the supermarket. At a local scale, however, we can find some exceptions. In the north, for instance, several areas have more cardmembers than their neighborhood: Komaba 3-chome, Shoto 1-chome,

Dogenzaka 2-chome, Shibuya 1-chome, and Shibuya 4-chome. In contrast, Dogenzaka 1-chome has fewer members than its surrounding areas. These kinds of spatial irregularities provide regional information which is useful for market analysis. A local concentration of customers, which is represented as a small peak in a surface, may indicate that the goods provided at the supermarket A especially suit the taste of residents in the area. A pit in consumer distribution suggests the existence of competing supermarkets.

Fig. 10. Average distribution of cardmembers shopping at the supermarket A (1/day·household).

These irregularities, however, cannot be accepted immediately. Market structure changes constantly, and irregular patterns often appear only by chance. We should focus on the stable spatial pattern in market analysis to understand the fundamental structure of the market.

To this end, we applied the method proposed in the previous sections to the data. Our objective was to evaluate the stability of the market and to extract stable spatial elements from the market structure. We constructed a TIN (Triangular Irregular Network) based on the representative points of oazas to obtain continuous surfaces representing the daily market structure. To evaluate the market stability we calculated three agreement

functions, that is, complete, partial, and generalized agreement functions, and their integral indices. In the partial agreement function the parameter μ was set to 0.9. Concerning the functions we show only the distribution of generalized agreement function for economy of space (Figure 11). The other functions can be easily derived from the generalized agreement function because it is a generalized version of the others.

Fig. 11. Generalized agreement function for the daily distribution of cardmembers shopping at the supermarket A, integrated by θ at each location.

The complete, partial, and generalized agreement indices are 0.0487, 0.7310 and 0.9409, respectively. The partial and generalized agreement indices are relatively large, which implies global stability of the market structure. The small complete agreement index, on the other hand, supports our concern mentioned earlier: its definition is too strict for practical use. The partial and generalized agreement indices are more flexible and informative.

The generalized agreement function presents the spatial variation of market stability (Figure 11). The function is large near the supermarket, and it decreases with the distance from the supermarket. This is mainly because the market stability depends on the number of customers. The market structure becomes stable if there are many customers, as seen

in the neighborhood of the supermarket. If there are only a few customers, on the other hand, the market structure is prone to change drastically.

Comparing Figures 10 and 11, we find some local peaks in the customer distribution around which the generalized agreement function is small: Komaba 3-chome, Shoto 1-chome, and Dogenzaka 2-chome. This indicates instability of market structure in these areas. The local peaks may have appeared only by chance.

To test this hypothesis, we extracted α-peak regions, α-pit regions and β-monotonic lines from the data (Figure 12). Parameters α and β were both set to 0.95, and the area of α-peak and α-pit regions was limited to five percent of the study area.

Fig. 12. α-peak regions, α-pit regions and β-monotonic lines detected in the daily distribution of cardmembers shopping at the supermarket A. β-monotonic lines are grouped into polygons.

Figure 12 supports our hypothesis. Only two α-peak regions were detected, one near the supermarket A (rank 1) and the other in the east of Shibuya station (rank 2). We tried several parameter values but obtained the same result. From this we conclude that the local peaks of Komaba 3-chome, Shoto 1-chome, and Dogenzaka 2-chome found in Figure 10 are not significant; the supermarket A is not strong particularly in these areas

compared with their neighborhood.

The α-peak region in the east of Shibuya station covers Shibuya 1-chome and 4-chome areas. This is probably because people with high incomes live in these areas who prefer high-class supermarkets like the supermarket A. The size of this α-peak region is relatively large, which reflects the locational instability of the peak. A local peak of customer distribution exists constantly in the α-peak region, but it moves over time within the region, probably between Shibuya 1-chome and Shibuya 4-chome areas. Though it is certain that the two regions have more customers than their surrounding areas, there is no significant difference between the two regions.

The α-pit region in the west of Shibuya station corresponds to the sudden decrease of cardmembers in Dogenzaka 1-chome (see Figure 10). Since there are only a few supermarkets around this area, the α-pit region seems to indicate the disagreement between the taste of people in this area and the goods of the supermarket A.

Let us finally discuss β-monotonic lines which represent the stable and monotonic market areas. Though originally extracted as lines, they were simplified into polygons in the figure. The polygons are ellipses rather than circles: customers decrease monotonically in the northwest and southeast directions, while they fluctuate in the northeast and southwest directions. Comparing Figures 10 and 12, we can consider three causes for this: 1) there are competing supermarkets in the southwest area, near railway

stations; 2) people with high incomes live in the northwest and southeast areas; 3) supermarkets around Ebisu station provide low-priced foods, which do not fit the taste of people there.

5. CONCLUSION

In this paper we have developed a method for analyzing the similarity among surfaces defined in the identical region. The method evaluates the similarity among surfaces with respect to their spatial configuration, and detects spatial structures shared by the surfaces. Four functions are proposed to measure the surface similarity: the complete, partial, spatially-extended, and generalized agreement functions. The integrals of these functions, which are called agreement indices, indicate the global similarity among surfaces in a region. The functions and indices show 'to what extent' surfaces are similar. To describe 'how' surfaces are similar, we proposed three types of spatial objects: α-peak regions, α-pit regions and β-monotonic lines. They reveal the spatial structures shared by surfaces, which is useful especially in exploratory spatial analysis. To test the validity of the method, we analyzed the daily market structure of a supermarket in Japan. The empirical study yielded some interesting findings that help us understand the spatial aspect of market structure.

In this paper we proposed three types of spatial objects to represent the spatial

structures shared by surfaces. Generalizing their underlying concepts, we obtain a wider variety of spatial objects potentially applicable to further analysis of surface similarity.

The α-peak and α-pit regions are both spatial regions containing points of a certain type that characterize surfaces. This implies that we can consider any type of points on surfaces other than peaks or pits, and calculate the regions in which they are contained. For instance, if cols (saddle points) are important in analysis, we can detect the regions that contain cols of many surfaces. Given the type of points, we can calculate their containing regions by the computational algorithm developed in this paper.

The β-monotonic line, on the other hand, is a set of points on all of which many surfaces share the same slope function. This suggests that, at least in theory, we can consider any spatial object on which many surfaces have the same slope function, because any spatial object is defined as of a set of points. Examples include the region in which many surfaces face north, the point on which many surfaces increase in a certain direction, and so forth. Extension in this direction, however, requires discussion about the desirable properties of spatial objects and development of computational algorithms to extract the objects. The latter is critical because it is practically meaningless to consider spatial objects that cannot be detected efficiently in computer environment. Though some objects may be detectable by a slight modification of our algorithm, it would apply only to limited cases. General computational algorithms of wider application are indispensable for

future research.

Acknowledgment

The authors are grateful to the supermarket A for providing the shopping histories of cardmembers.

LITERATURE CITED

Bailey, T. C. and A. C. Gatrell (1995). *Interactive Spatial Data Analysis*. London: Taylor & Francis.

Bracken, I. (1993). "An Extensive Surface Model Database for Population-Related Information." *Environment and Planning B,* **20**, 13-27.

Bracken, I. and D. Martin (1995). "Linkage of the 1981 and 1991 UK Censuses Using Surface Modelling Concepts." *Environment and Planning A,* **27**, 379-390.

Cressie, N. (1993). *Statistics for Spatial Data*. New York: John Wiley.

Etzelmuller, B. (2000). "On the Quantification of Surface Changes Using Grid-based Digital Elevation Models (DEMs)." *Transactions in GIS*, **4**, 129-143.

Fiacco, A. V. and G. P. McCormick. (1968). *Nonlinear Programming: Sequential Unconstrained Minimization Technique*. New York and Toronto: John Wiley.

Gill, P. E., W. Murry, and M. H. Wright. (1981). *Practical Optimization*. London: Academic Press.

Hutchinson, N. F. (1989). "A New Procedure for Gridding Elevation and Stream Line Data with Automatic Removal of Spurious Pits." *Journal of Hydrology*, **106**, 211-232.

Isaaks, E. H. and R. M. Srivastava. (1989). *An Introduction to Applied Geostatistics*. New York: Oxford University Press.

Megiddo, N. (1983). "Linear-Time Algorithm for Linear Programming in R^3 and Related Problems." *SIAM Journal on Computing*, **12**, 759-776.

Nakaya, T. (1997). "Statistical Inferences in Bidimensional Regression Models." *Geographical Analysis*, **29**, 169-186.

Okabe, A. (1982). "Qualitative Method of Trend Curve Analysis." *Environment and Planning A*, **14**, 623-627.

Pike, R. J. (1988). "The Geometric Signature: Quantifying Landslide-Terrain Types from Digital Elevation Models." *Mathematical Geology*, **20**, 491-511.

Preparata, F. P. and M. I. Shamos. (1985). *Computational Geometry: An Introduction*. New York: Springer-Verlag.

Sadahiro, Y. (2001a). "Analysis of Surface Changes Using Primitive Events." *International Journal of Geographical Information Science*, **15**, 523-538.

Sadahiro, Y. (2001b). "Spatio-temporal Analysis of Surface Changes by Tessellations." *Geographical Analysis*, **33**, 312-329.

Sadahiro, Y. (2002). "A Graphical Method for Exploring Spatiotemporal Point Distributions." *Cartography and Geographical Information Science*, **29**, 67-84.

Sadahiro, Y. (2003). "Stability of the Surface Generated from Distributed Points of Uncertain Location." *International Journal of Geographical Information Science*, to appear.

Tobler, W. (1994). "Bidimensional Regression." *Geographical Analysis*, **26**, 186-212.

Skyum, S. (1991). "A Simple Algorithm for Computing the Smallest Enclosing Circle." *Information Processing Letters*, **3**, 121-125.

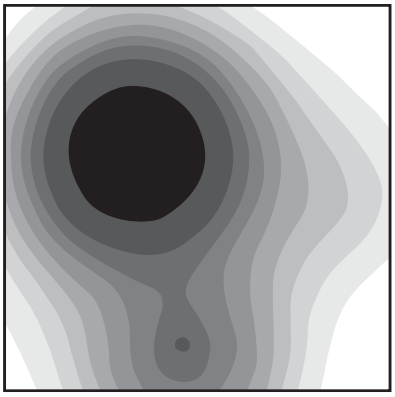

Age group 1: under 20

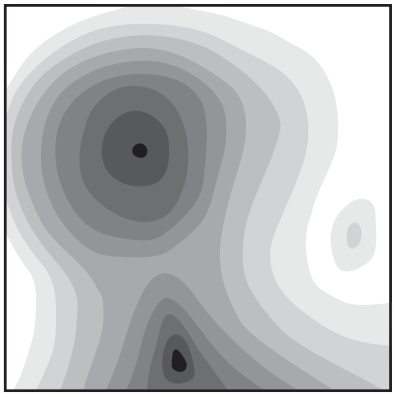

Age group 2: 20-40

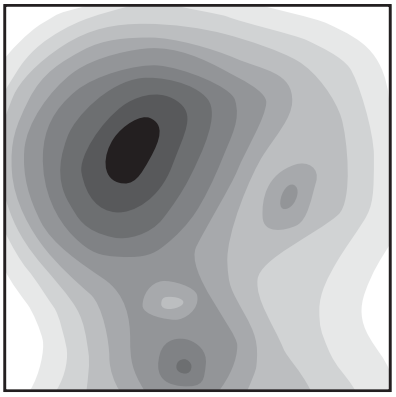

Age group 3: over 40

Figure 1

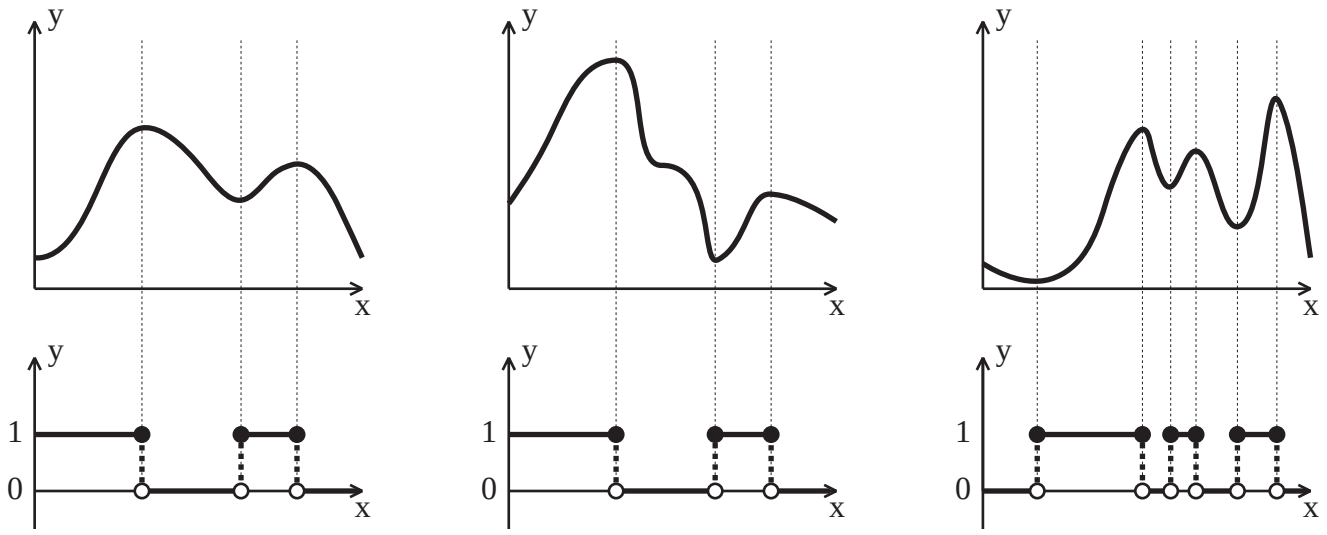

Figure 2

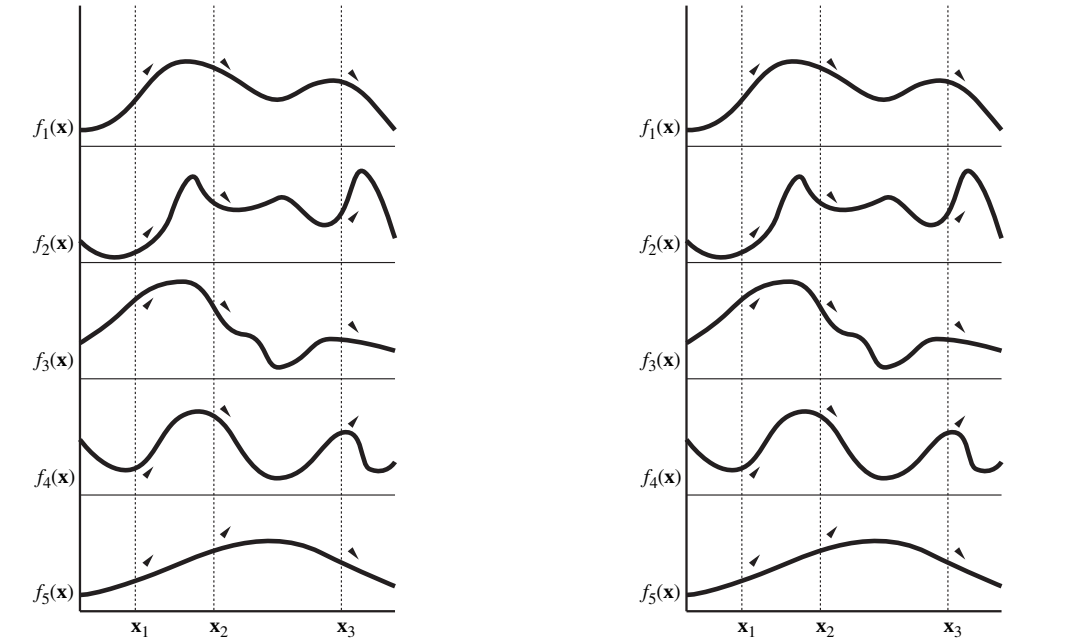

$\eta(\mathbf{x}, \theta; F)$ 1 0 0

(a)

$\eta_P(\mathbf{x}, \theta, \mu; F)$ 1 1 0

(b)

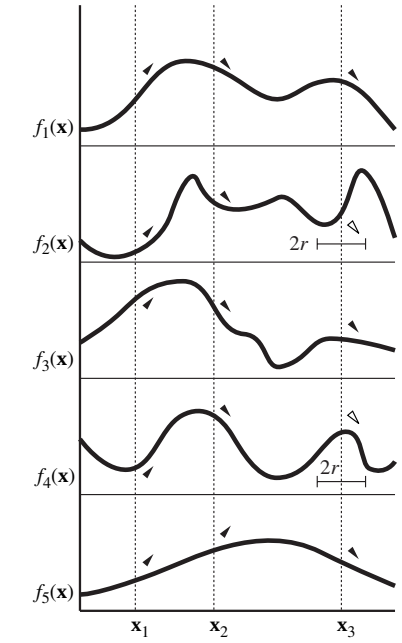

$\eta_s(\mathbf{x}, \theta, r; F)$ 1 0 1

(c)

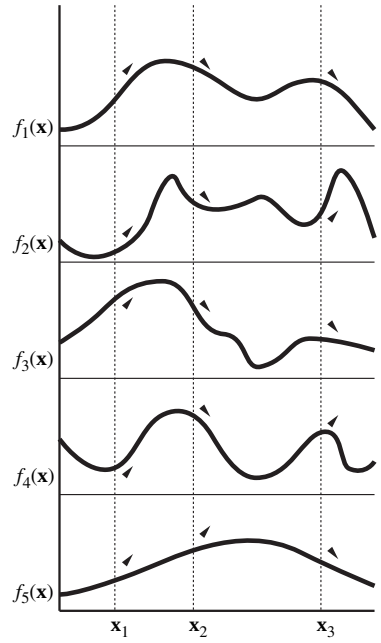

$\eta_g(\mathbf{x}, \theta; F)$ 1.0 0.8 0.6

(d)

Figure 3

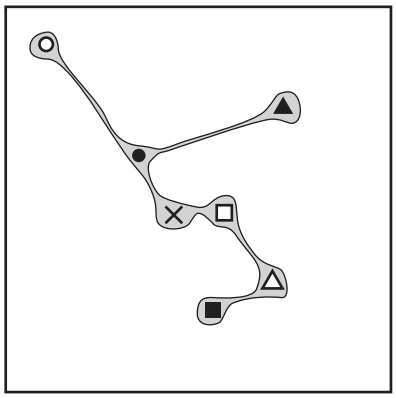

Figure 4

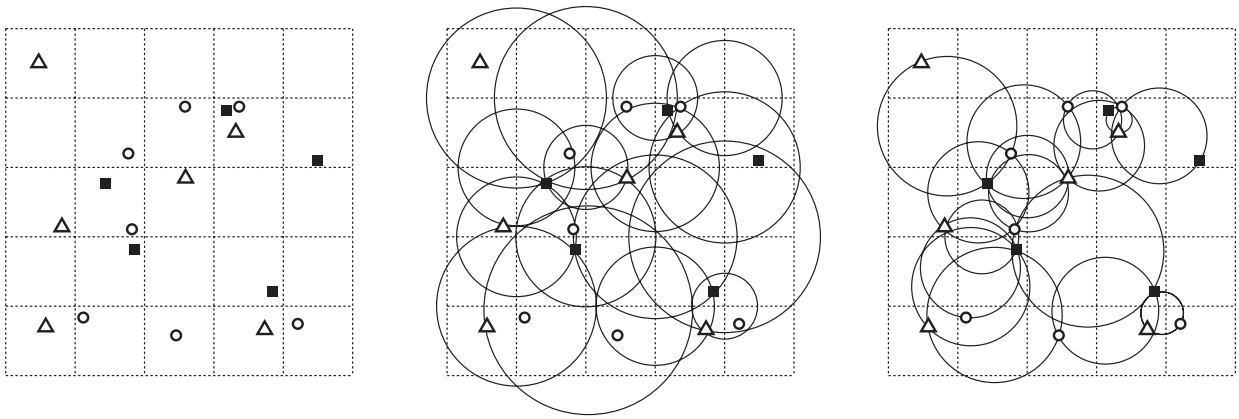

(a) (b) (c)

Figure 5

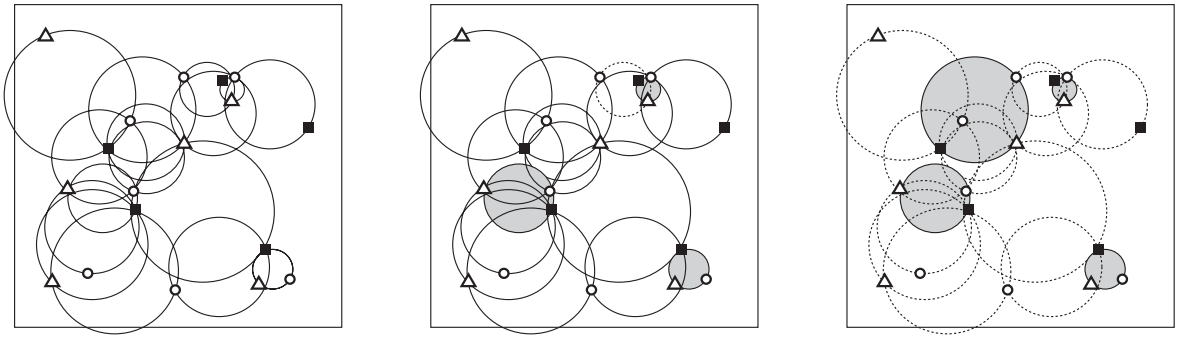

(a) (b) (c)

Figure 6

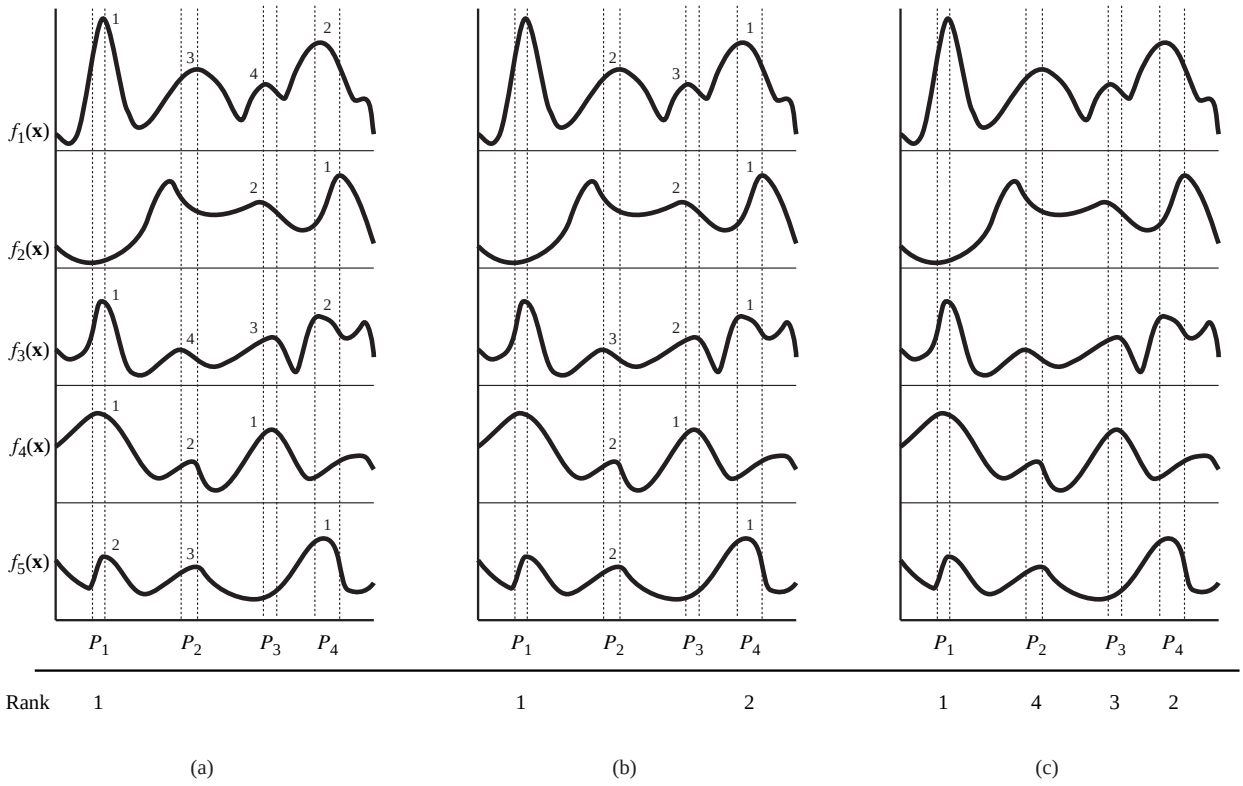
$f_1(\mathbf{x})$
$f_2(\mathbf{x})$
$f_3(\mathbf{x})$
$f_4(\mathbf{x})$
$f_5(\mathbf{x})$
P_1 P_2 P_3 P_4
Rank 1
1 2
1 4 3 2
(a)
(b)
(c)

Figure 7

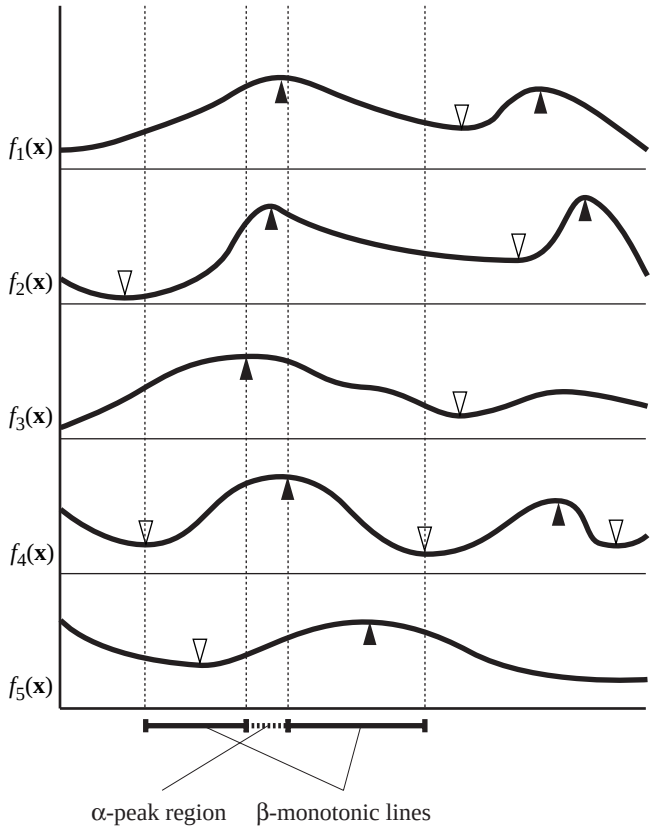
$f_1(\mathbf{x})$
$f_2(\mathbf{x})$
$f_3(\mathbf{x})$
$f_4(\mathbf{x})$
$f_5(\mathbf{x})$
α-peak region
β-monotonic lines

Figure 8

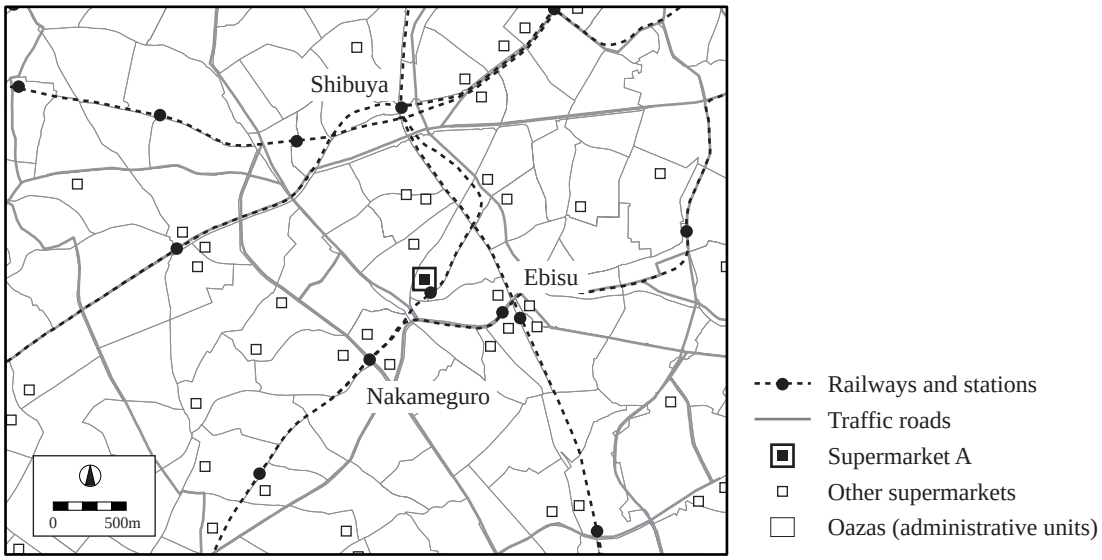
Shibuya
Ebisu
Nakameguro
0
500m
Railways and stations
Traffic roads
Supermarket A
Other supermarkets
Oazas (administrative units)

Figure 9

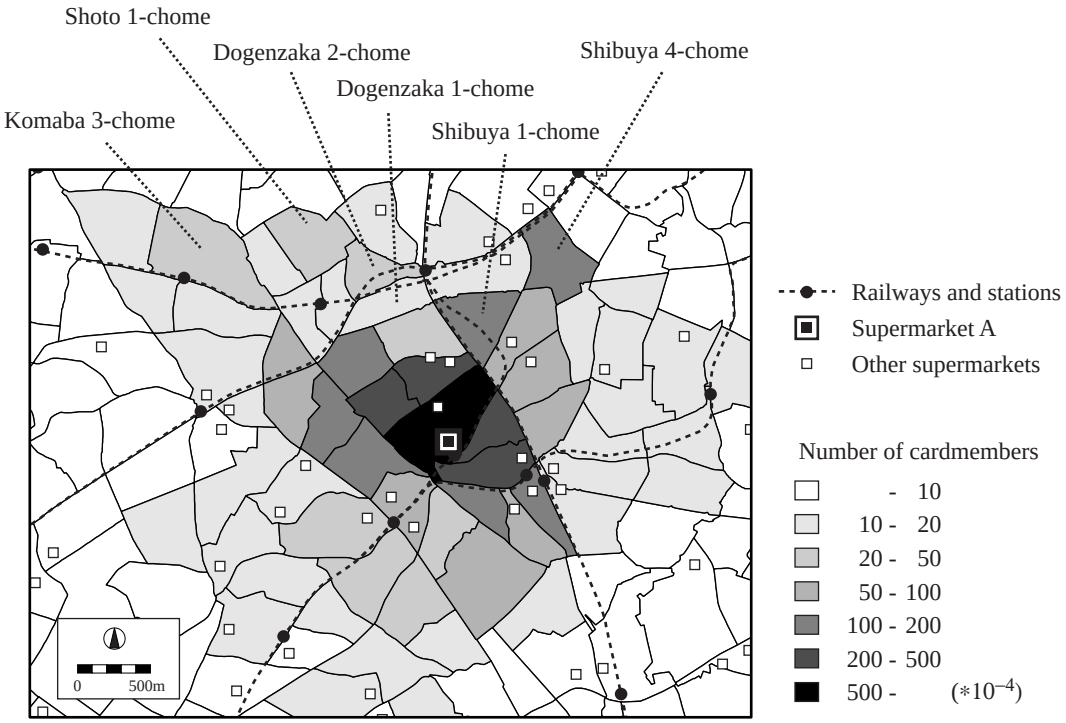
Shoto 1-chome
Dogenzaka 2-chome
Shibuya 4-chome
Dogenzaka 1-chome
Komaba 3-chome
Shibuya 1-chome
0
500m
Railways and stations
Supermarket A
Other supermarkets
Number of cardmembers
- 10
10 - 20
20 - 50
50 - 100
100 - 200
200 - 500
500 -
(∗10−4)

Figure 10

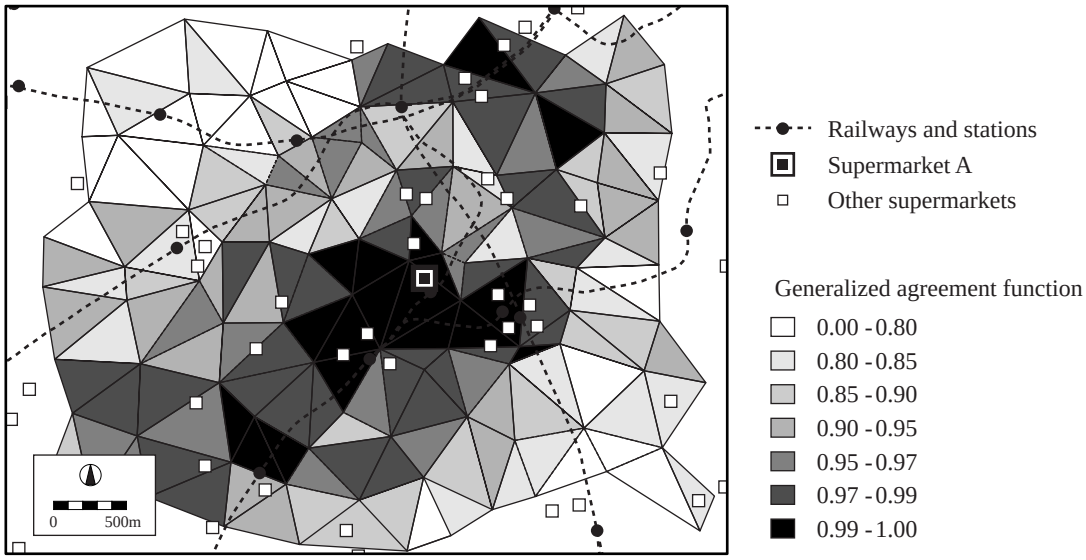
Railways and stations
Supermarket A
Other supermarkets
Generalized agreement function
0.00 - 0.80
0.80 - 0.85
0.85 - 0.90
0.90 - 0.95
0.95 - 0.97
0.97 - 0.99
0.99 - 1.00
0
500m

Figure 11

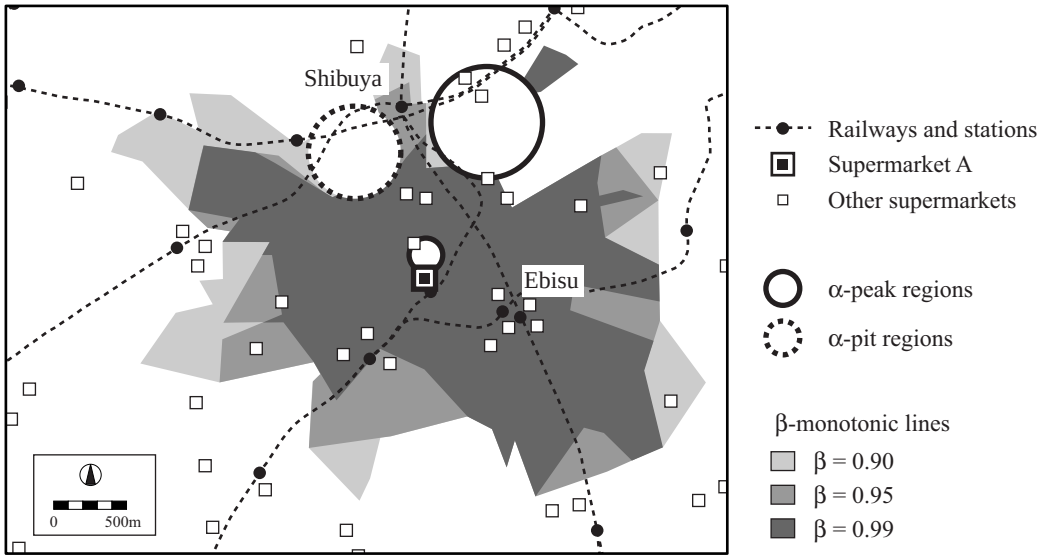
Shibuya
Ebisu
0
500m
Railways and stations
Supermarket A
Other supermarkets
α-peak regions
α-pit regions
β-monotonic lines
β = 0.90
β = 0.95
β = 0.99

Figure 12